Cold Regions Science and Technology, 11 (1985) 155–170
Elsevier Science Publishers B.V., Amsterdam – Printed in The Netherlands

EXPERIMENTAL STUDIES ON ICE SHELLS IN ASAHIKAWA

Tsutomu Kokawa
Department of Art and Technology, Hokkaido Tokai Univ., Asahikawa (Japan)

(Received August 13, 1984; accepted in revised form February 7, 1985)

ABSTRACT

An ice shell is thin, and its structural material is snow-ice. It may be an efficient form of instant shelter for snowy and cold regions. This paper describes two field studies on ice domes carried out in Asahikawa. The first one is an investigation on the creep collapse of a 5-m span model under a concentrated load acting on a circular area at the apex. Normal displacements and temperatures were measured up to the collapse. Experimental collapse time was examined, introducing the classical creep buckling value of a completely spherical shell under uniform external pressure. The second study deals with both the construction technique and the creep test of a 10-m span model. The construction technique consists of: (1) inflating a membrane bag covered with rope, (2) spraying it with snow and water, (3) solidifying the snow-ice sherbet on it, and (4) removing the bag and rope for reuse. Subsequently, a creep test was carried out under snow load, and its structural behaviour up to the collapse was examined. Based on the results of these studies, the production of 20–30-m span ice shells may be practicable.

1. INTRODUCTION

Asahikawa is located in the center of Hokkaido in Japan. The physical environment of Asahikawa district becomes severe in winter. According to meteorological data for the past thirty years (Sapporo Meteorological Agency, 1982), the average air temperature in January and February is about −8°C, the yearly total number of ice days is 80, and the yearly mean maximum snow depth is 90 cm. Aiming at the production of ice shells with spans from 20 to 30 m, which could be used for a variety of expedient shelters, such as sport-leisure centers, festival halls, warehouses, car sheds, etc. in this environment, the author has been making experimental and theoretical investigations on both the structural safety and the construction method of the ice shell using scale models. Experiments and analyses on ice domes with 60-cm span under short-term loading (Kokawa and Hirasawa, 1983), experiments on ice domes with 60-cm (Kokawa, 1983a), 2-m (Hirasawa and Kokawa, 1984), 5-m (Kokawa, 1983b), and 10-m spans under long-term loading, and the axisymmetric creep buckling analysis of ice domes (Kokawa, 1984a), were conducted together with investigations on the structural safety. At the same time, an ice shell construction method proposed by the author has been tested for models with spans of 5 m and 10 m (Kokawa, 1984b).

The ice shell is thin, and its structural material is snow-ice. The ice shell may be considered a contemporary "igloo" or "kamakura". It may be a suitable method for using ice and snow-ice as structural material and may provide an efficient architectural solution to certain problems in the snowy and cold regions. The snow dome with a 10-m span was constructured by blowing milled snow over an inflatable hemisphere by a Peter miller (Mellor, 1968). Stanley and Glockner (1975a, 1975b, 1977) carried out, at first, an experimental creep study on reinforced ice domes with a 2-m span produced by spraying water onto an inflatable membrane. The same construction method was also used for ice structures in Europe (IL 9, 1976; Isler, 1979) and in Japan.

0165-232X/85/$03.30

However, the ice shell with a 20–30-m span has not yet been produced because there still exist many problems to be solved related to the structural safety and the construction technique. This paper describes two field studies carried out at Hokkaido Tokai University in Asahikawa. One is an experimental study on the creep collapse of a 5-m ice dome during the winter of 1981–1982. The other one is a field study on both the construction method and the creep test of a 10-m span ice dome during the winter of 1983–1984.

2. THEORETICAL BACKGROUND

As is generally known, thin shell structures have usually enough stiffness and load carrying capacity in comparison with their own weight, and are used to span wide roofs.

By comparing the mechanical properties of flat plates and shells, it can be understood how shell structures have superior structural efficiency. Figure 1 shows configurations of a spherical shell and a flat plate, each with 30 cm thickness and 30 m diameter. Comparisons of stress and deflection are made at the central point of these structures. The methods of computation are based on membrane theory in the case of the shell, and thin plate theory in the case of the flat plate (Timoshenko and Krieger, 1959). The results are as follows:

(1) $\sigma_s/\sigma_p = 1/37$, where σ_s, σ_p are the stress of the shell and the plate, respectively. With a vertical unit load of $q = 500$ kg/m^2, σ_s becomes 1.8 kg/cm^2 in compression. This value is about 1/25th of the uniaxial compression strength of snow-ice (Kokawa and Hirasawa, 1983);

(2) $\delta_s/\delta_p = 1/273$, where δ_s, δ_p are the vertical deflections of shell and plate, respectively. If Young's modulus E is 5000 kg/cm^2, δ_s becomes 7.5 mm.

Consequently, even if the structural material does not have enough strength and stiffness, like snow-ice, it is possible to cover a relatively large span by using a shell structure.

3. STUDY ON CREEP COLLAPSE OF 5-M ICE DOME

As described in the section 2, the strength of an ice shell may be sufficient for some given loads over a short period. However, since the snow-ice creeps, it is important to investigate the creep behaviour of an ice shell which will experience loads for a long time.

According to the experimental study on the creep buckling of 60-cm span models (Kokawa, 1983a) under constant load and temperature, similar to high-temperature metal vessels (Gerdeen and Sazawal, 1974), the deformation grows with time through the primary, secondary and tertiary stages of creep, and then the structure collapses. After all, the phenomenon of the creep buckling collapse is governed by a critical time as well as a critical load. Therefore, for appreciable lifetimes and given any load, the creep

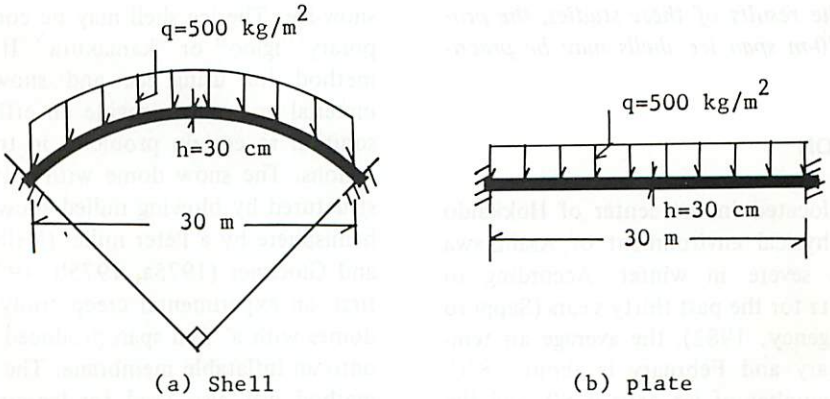

Fig. 1. Comparison of structural efficiency between shell and plate.

buckling collapse should be avoided. Understanding of this phenomenon holds the key to the application of ice shells.

3.1 Construction of test model

The test model has a 5-m diameter and a 90-degree open angle, as shown in Fig. 2. Such a model, with simple geometry, facilitates analysis of the experimental results. The model was constructed as follows.

(1) The boundary of the synthetic fiber membrane is fixed and sealed by bolts at the side wall of a reinforced concrete foundation ring with a 5-m inside diameter. In the fabrication of the membrane which serves as formwork for the erection of the desired spherical dome, 24 spherical triangular segments

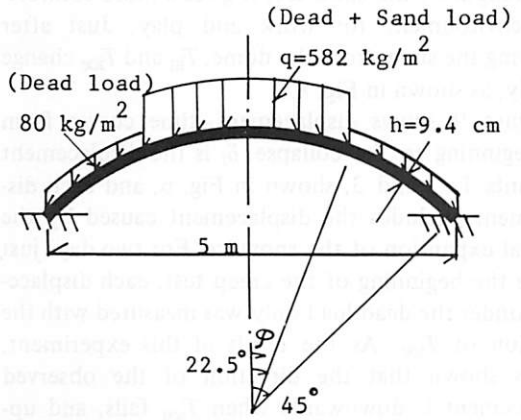

Fig. 2. Analytical model of 5-m span ice dome.

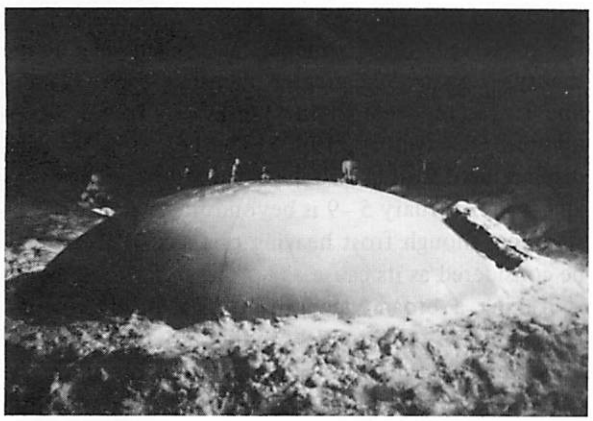

Fig. 3. Air-inflated membrane as formwork.

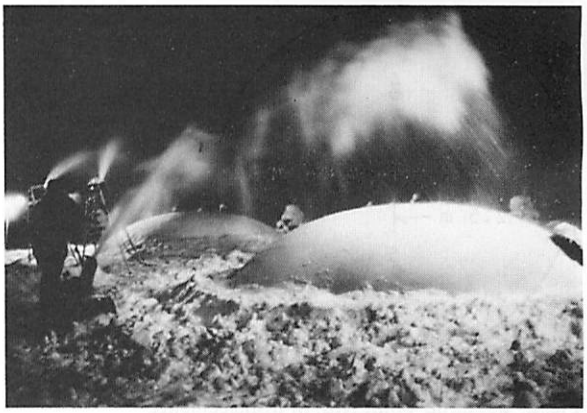

Fig. 4. Blowing snow and spraying water on the membrane.

Fig. 5. Loading.

were cut, and were joined by means of welding along the longitudinal line.

(2) The membrane is air-inflated by a voltex blower, and the inner pressure is held at 6 cm water head by a pressure controlling machine, as shown in Fig. 3.

(3) Snow is blown onto the membrane by a rotary snow-plow, and tap water is sprayed on the snow with an adjustable nozzle, as shown in Fig. 4. As a result of this operation, snow-ice sherbet is produced on the membrane, and it freezes hard some time later. The application of snow and water is repeated up to the desired thickness.

(4) After the snow-ice freezes and hardens, the membrane is deflated and removed. The membrane can then be reused.

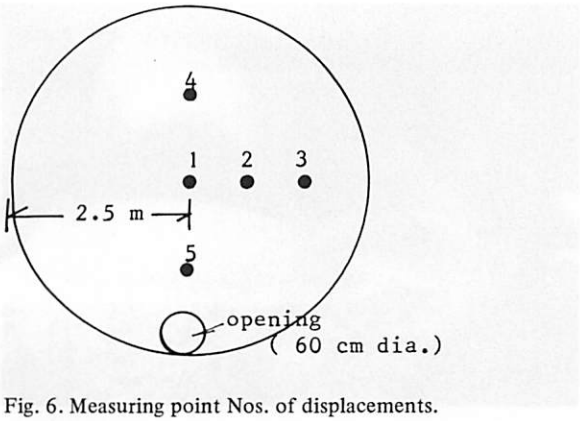

Fig. 6. Measuring point Nos. of displacements.

3.2 Method of creep test

Axisymmetric distributed vertical load was applied to the test dome by placing 20-kg sand bags on a circular area ($\varphi \leqslant 22.5°$) concentric with the apex, as shown in Fig. 5. The total sand load on the dome was 2 tons from the beginning to January 26, 1982, and 3 tons from January 26 to the collapse, respectively. Vertical loads shown in Fig. 2 are determined by assuming that the density of the snow-ice is 0.85 g/cm^3, the total sand load is 3 tons, and the average shell thickness is 9.4 cm.

Figure 6 shows the location of the points for measuring the normal displacements. Each displacement was measured by a displacement transducer which was set up at the top of an H-shaped column, as shown in Fig. 7. Outside, inside and snow-ice temperatures were measured using copper–constantan thermocouples. Displacements and temperatures were recorded automatically by a programmable data logger every 2 or 3 hours.

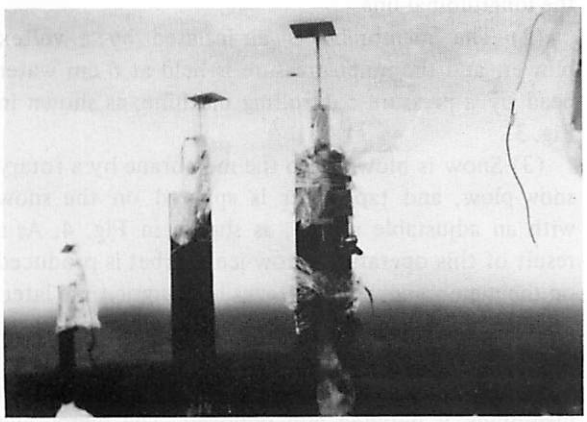

Fig. 7. Installation of displacement transducer.

3.3 Results and discussions

Figure 8 shows three temperature–time curves during the whole experiment. T_{out}, T_{in} and T_{ice} are outside, inside and snow-ice temperatures, respectively. The average values of T_{out}, T_{in} and T_{ice} are $-9.65°C$, $-3.90°C$ and $-5.53°C$, respectively. Under the condition where the dome has a small opening and some snow cover like in this test, T_{in} and T_{ice} are about 5°C higher and change more slowly than T_{out}, due to the thermal insulation effect of the snow cover and the snow-ice. Although a rise in T_{in} and T_{ice} is not desirable, because this decreases the strength of the snow-ice, it gives a more comfortable environment for work and play. Just after removing the snow from the dome, T_{in} and T_{ice} change sharply, as shown in Fig. 8.

Figure 9 shows displacement–time curves from the beginning to the collapse. δ_i is the displacement at points 1, 2 and 3, shown in Fig. 6, and each displacement excludes the displacement caused by the thermal expansion of the snow-ice. For two days just before the beginning of the creep test, each displacement under the dead load only was measured with the variation of T_{ice}. As the result of this experiment, it was shown that the direction of the observed displacement is downwards when T_{ice} falls, and upwards when it rises. It was concluded that the displacement was caused by the thermal expansion of the snow-ice. The computed thermal expansion coefficients of the snow-ice at each point, based upon the observed displacements and shell membrane theory, is about 50% greater than that of polycrystalline ice as reported in the literature (Tokyo Astronomical Observatory, 1982). The behaviour of each displacement during two days just after the beginning and from February 5–9 is beyond the author's understanding, though frost heaving or thermal effect may be considered as its cause.

Taking a broad view, the central displacement–time curve is qualitatively similar to the behaviour under constant load and temperature. That is, the deformation grows linearly with time during from the beginning to February 17, when the displace-

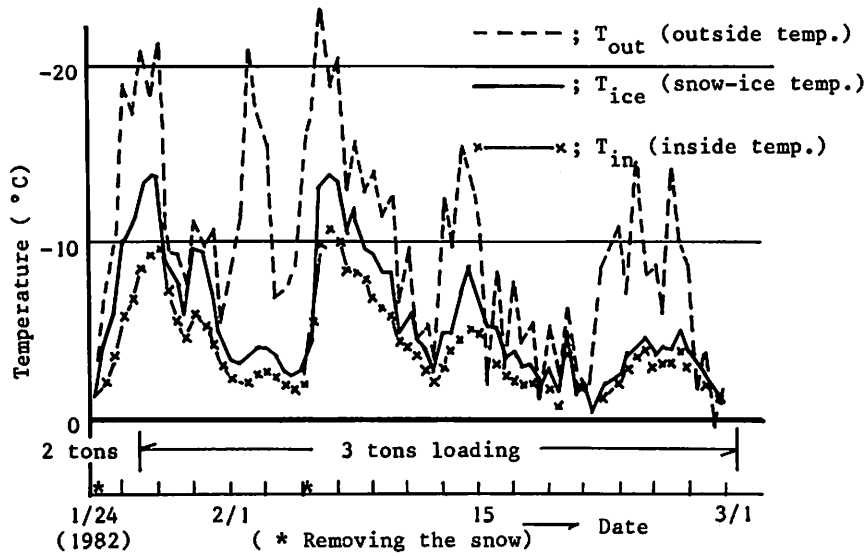

Fig. 8. Temperature–time curves.

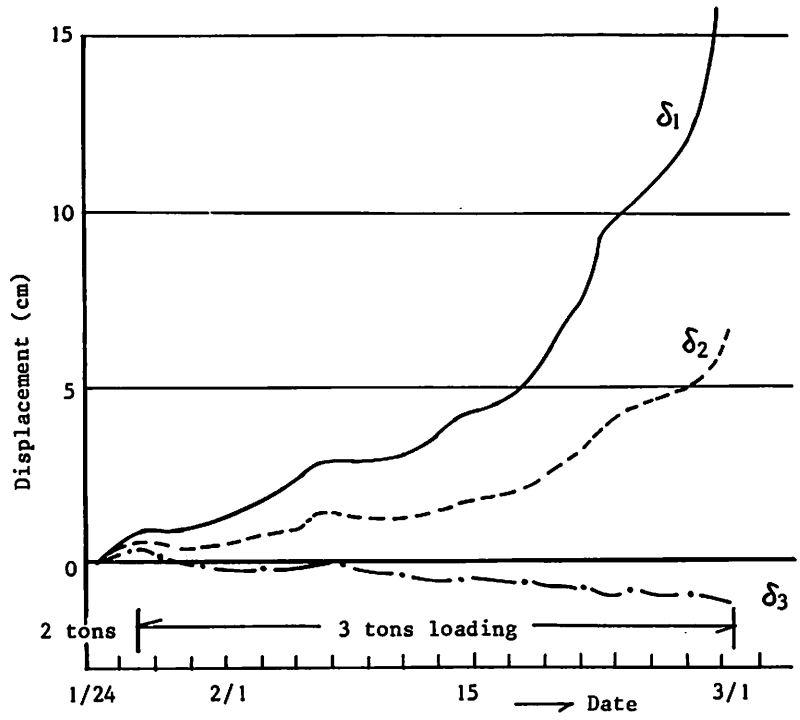

Fig. 9. Displacement–time curves.

ment reaches half of the shell thickness and thereafter accelerates up to creep collapse.

Assuming that the comstitutive law of the snow-ice is approximately obeyed in accordance with linear Newtonian flow (eqn. 1) because of low stress in the model as shown in Fig. 10, and there is no volume change under creep, and linear shell theory is valid. The normal deformation and the stresses in this

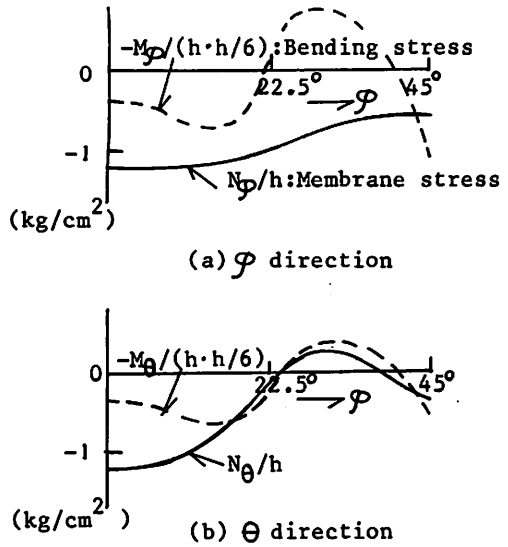

Fig. 10. Theoretical stress distribution.

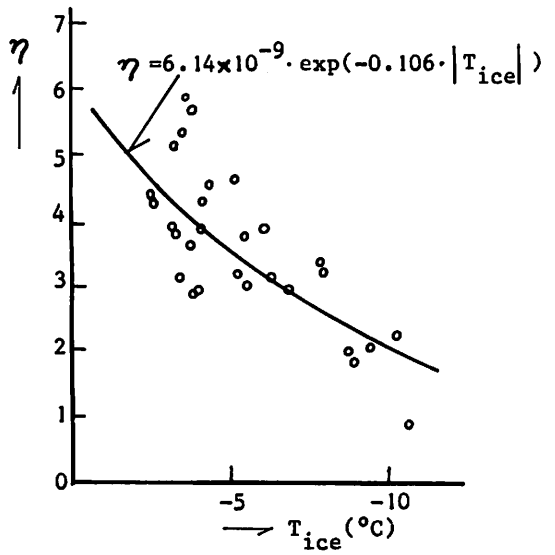

Fig. 11. Creep coefficient η as function of T_{ice}.

model (Fig. 2) were computed by means of a previously described method (Kokawa and Hirasawa, 1983). Equation (1) is given by

$$\dot{e} = \eta\,\sigma \tag{1}$$

where $\dot{e}$, η and σ are strain rate, creep coefficient and stress, respectively, under uniaxial compression or tension. Figure 11 represents the η–T_{ice} relation from February 1–17 when each observed displacement seems to be not affected so much by frost heaving and geometrical nonlinearity. η is evaluated as follows.

First, the function f is defined as

$$f = \sum_{i=1}^{3} [cy_i - (\Delta\delta_i + d)]^2 \tag{2}$$

where i is from 1 to 3, and y_i and $\Delta\delta_i$ are the theoretical displacement velocity (cm/sec) for $\eta = 1$ (cm^2/kg·s^{-1}), and the observed incremental displacement (cm) over half a day, respectively, at point i. In this analysis, y_1, y_2 and y_3 are taken as 728, 541, and −51.7, respectively. Then c was determined so as to minimize the function f with respect to c and d. Finally, η is computed as

$$\eta = c/(60\cdot 60\cdot 12)\ \ (\mathrm{cm^2/kg\cdot s^{-1}}) \tag{3}$$

As shown in Fig. 11, η is directly related to T_{ice}, which is the average for half a day. The present data can be represented by the empirical relation

$$\eta = A\exp(-B|T_{ice}|) \tag{4}$$

The values of A and B were determined by a least-squares fit as $6.14\cdot 10^{-9}$ and 0.106, respectively. The value of η was somewhat higher than the values gives by the creep test reported by (Mellor and Smith, 1966).

Now, in order to evaluate the experimental collapse time and load, let us introduce the dimensionless experimental creep buckling value α_{cr}, defined by

$$\alpha_{cr} = (\eta\, t\, q)_{cr} = \eta_{av}\, t_{cr}\, q \tag{5}$$

where η_{av} is obtained by substituting the average T_{ice} during the whole experiment (−5.53°C) in eqn. (4). t_{cr} and q are the collapse time and the unit load, respectively. In this case, each value is taken as follows.

$\eta_{av} = 3.42\cdot 10^{-9}$ (cm^2/kg·s^{-1})

$t_{cr} = 34.5$ (d), $\quad q = 582$ (kg/m^2)

Then, from eqn. (5), $\alpha_{cr} = 5.93\cdot 10^{-4}$. Subsequently, a dimensionless creep buckling value α_{cr0} is introduced as a standard value. α_{cr0} is obtained by transforming the classical buckling formula of a complete spherical shell under uniform pressure (Timoshenko and Gere, 1961). α_{cr0} is expressed by

$$\alpha_{cr0} = 4/(3\lambda^2) \quad (6)$$

λ is radius/thickness, 37.7, so that $\alpha_{cr0} = 9.38 \cdot 10^{-4}$. Finally, α_{cr}/α_{cr0} is 0.63. This value is in the range of the previous test results (Kokawa, 1983a). According to the author's analysis with respect to axisymmetric creep buckling of ice domes (Kokawa, 1984a), it is shown that the α_{cr}/α_{cr0} at uniform loading is larger than that at the concentratedly distributed load. However, even taking into account the above, the ice shell with a 30-m span is in danger of creep buckling collapse in a short period, i.e., one or two months. Consequently, a procedure for increasing the effective shell thickness by a humped effect will be described in section 4. This should be done to delay the occurrence of creep buckling collapse.

4. STUDY ON 10-M SPAN ICE SHELL

4.1. Construction test

4.1.1 Construction method

The ice shell should have the facility to be constructed rapidly, easily and economically to provide expedient structures during winter. By taking hints from the erection method of existing (glass fiber) reinforced concrete shell (Ishii, 1977), the author proposed a rapid, easy and economical construction technique of the ice shell, and had already applied this method successfully to some models with 5 m span.

Enlarging the scale of the model further, the author tried to construct an ice dome with a 10-m span by the following method.

(1) Polypropylene guy ropes are anchored to steel bars staked to the ground peripherally. The ropes are 9 mm in diameter, and the diameter, length and total number of the steel bars are 25 mm, 80 cm and 64, respectively. Subsequently, the peripheral foundation is made by snow and water. At this stage, steel bars are interbedded with the snow-ice foundation ring.

(2) A synthetic fiber membrane bag is placed on the ground as shown in Fig. 12. This membrane is fabricated by welder along the periphery after wrapping in two pieces of plane sheets with 10 m diameter. This bag is easy to fabricate because there

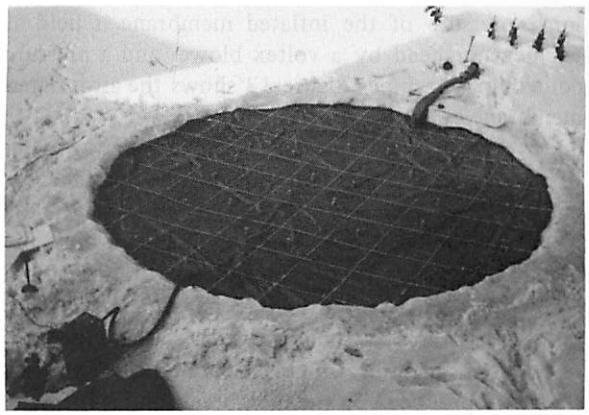

Fig. 12. Placing membrane on the ground.

is no three-dimensional cutting as in a sail or parachute.

(3) Each middle rope is laid orthogonally on the membrane and connected with the guy rope by a karabiner. Rope spacing in each direction is 1 m. Ropes play an important part not only in forming the shape of the air-inflated membrane, but also in providing the local curvature, or humped surface, thus increasing structural capacity, including resistance to creep buckling.

(4) About 25 pieces of styrene polypropylene (SP) boards (90 cm × 180 cm, 1.5 cm thickness) are placed at the narrow annular space between the periphery of the membrane and the foundation.

(5) After inflating the membrane bag in a short time by a sirocco fan (maximum air pressure 5 cm water head, maximum air flow 20 m^3/min), the

Fig. 13. Air-inflated membrane as formwork.

inner pressure of the inflated membrane is held at 6 cm water head by a voltex blower and a pressure controlling machine. Figure 13 shows the air-inflated membrane as a formwork.

(6) The space between the periphery of the membrane and the foundation ring is filled with snow and water, then frozen.

(7) As shown in Fig. 14, snow is blown onto the membrane by two rotary snow-plows with maximum throwing distances of 6 and 13 m, respectively, and tap water is sprayed on the snow by the adjustable nozzle. As a result of this operation, a snow-ice sherbet is produced on the membrane, and it is frozen hard some time later. Freezing and hardening speed of the snow-ice sherbet is primarily dependent on the outside air temperature. It is desirable for the outside temperature to be below −10°C, because if the temperature is above −10°C, the snow-ice sherbet melts rather than freezes when water is sprayed sequentially on the solid snow-ice. Figure 15 shows the outside temperature during construction. The application of snow and water are repeated up to the design thickness.

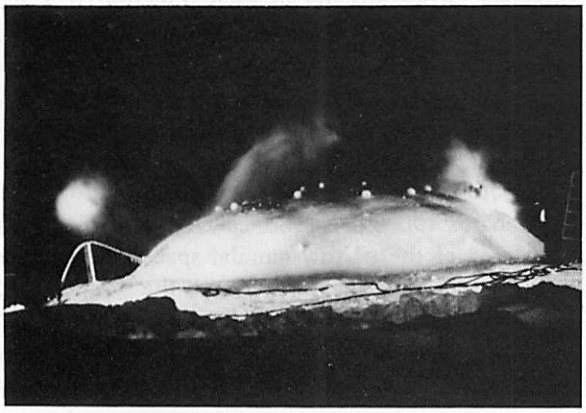

Fig. 14. Application of snow and water.

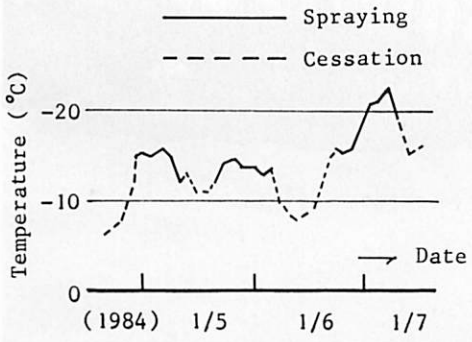

Fig. 15. Outside air temperature under snow and water spraying.

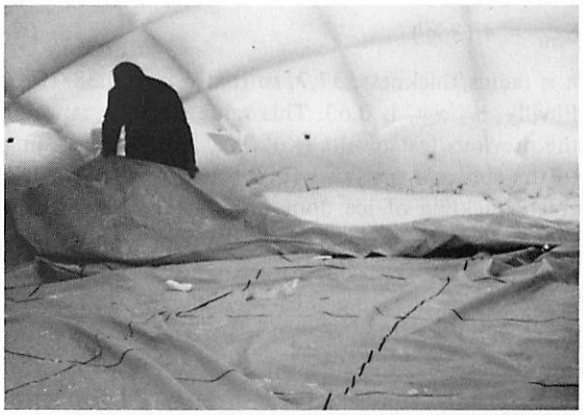

Fig. 16. Removing membrane from inside.

(8) After the snow-ice freezes and hardens, the membrane bag is deflated, as shown in Fig. 16, and then the SP boards, ropes and membrane are removed. The ice shell is then complete.

(9) SP boards, ropes and membrane bag can be reused. Repeating the above-mentioned operations from steps (1) to (8), additional structures can be constructed.

4.1.2 Consideration on the shape

The ice dome had a small circular opening with about 70 cm diameter. Three-dimensional coordinates at the inside intersecting points and the shell thickness at the major points were measured after the test dome had been finished. Figure 17 and Table 1 show

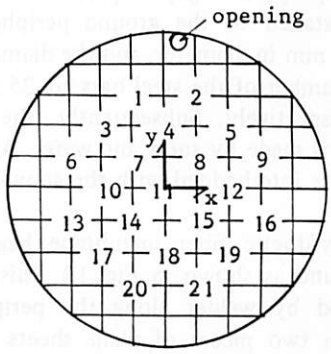

Fig. 17. Inside intersecting point Nos.

TABLE 1

Observed three-dimensional coordinate at each point

No.	x (cm)	y (cm)	z (cm)
1	− 96	307	143
2	101	307	139
3	−204	204	163
4	0	210	189
5	212	212	159
6	−318	107	144
7	−103	103	207
8	105	105	207
9	314	98	143
10	−208	0	192
11	0	0	222
12	214	0	192
13	−318	−104	149
14	−108	−108	208
15	106	−106	209
16	314	−114	148
17	−212	−212	165
18	0	−212	196
19	215	−215	165
20	−102	−320	148
21	97	−320	151

three-dimensional coordinates at the inside points of the test dome. Judging from the measurement, these points were nearly on a spherical surface, whose radius, computed by means of least-squares fitting, was 765 cm.

In this paper, a computational method to predict approximately the coordinate of the intersecting points is developed, and then the computed value is compared with the observed value for the central height of the test dome. In order to simplify the analysis, the following two assumptions are introduced.

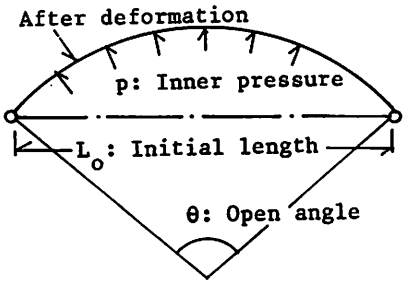

Fig. 18. Analytical model of a rope.

(1) The rigidity of the membrane is negligibly small in comparison with that of the ropes.

(2) Load carried from the membrane to the ropes is uniformly distributed normal pressure. As the result of assumption (2), the configuration of the rope after deformation becomes a circular arch as indicated in Fig. 18. Considering that the initial ropes are straight lines, the tension strain e of a rope is given by

$$e = \theta/[2\sin(\theta/2)] - 1 \tag{7}$$

where θ is the open angle after deformation. It is assumed that the constitutive law of the rope in tension is given by

$$N = a\, e^b \tag{8}$$

where N is the rope tension force, and a and b are material constants determined from the uniaxial test. Since the area enclosed by the ropes is 1 m × 1 m in this construction, N can be written as follows

$$N = 5\, H L_o/[2\sin(\theta/2)] \tag{9}$$

where H and L_o are air pressure and initial rope length, respectively. Units of N, H and L_o are kg, cm water head, and m, respectively. From eqns. (7–9), eqn. (10) is obtained as follows:

$$5\, H L_o/[2\sin(\theta/2)] = a\{\theta/[2\sin(\theta/2)] - 1\}^b \tag{10}$$

Equation (10) shows that θ is a function of H. In this case, the values of H, L_o, a and b are 6 cm water head, 10 m, 2126 kg and 1.188, respectively. Substituting these values into eqn. (10), θ becomes 98.8°. Consequently, the computed height of the central point, 2.3 m, is in fair agreement with the

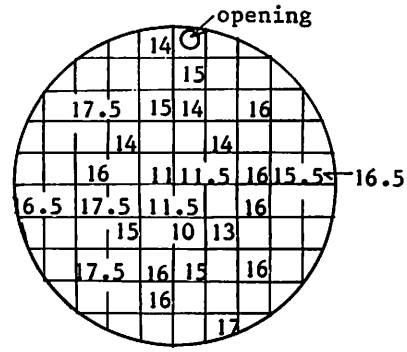

Fig. 19. Observed thickness of snow-ice plate at major points (cm).

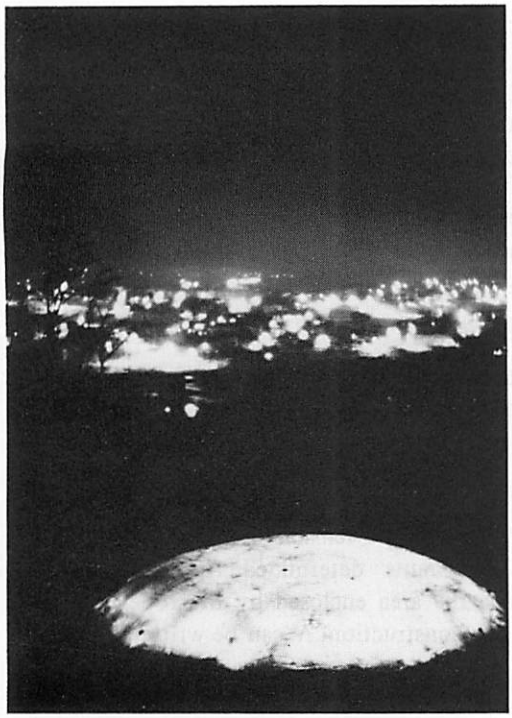

Fig. 20. Exterior view like a gigantic chandelier.

observed value, 2.22 m. The distribution of the observed thicknesses did not become uniform because of unskilled snow blowing during construction, as shown in Fig. 19. The central part was thinner than the other parts.

4.1.3 Aesthetic considerations

After the trial construction, an aesthetic presentation was carried out in the night using coloured lights inside the dome. Both the interior and the exterior were fantastic and beautiful. The interior had a brilliant space and its square grid pattern accented the curved surface. The exterior looked like a gigantic chandelier, as shown in Fig. 20.

4.1.4 Some problems

This construction method seems rapid, easy and economic. However, the following future problems have to be solved.

(1) *Temperature crack.* When the first water was sprayed again on the cold snow-ice after an interval of half a day, temperature cracks formed. This seemed to be caused by the difference in temperatures between the water and the snow-ice. Since these cracks are not propagated widely through the structure, it neither gives rise to general failure during construction, nor affects creep stability, since the dome is in a compressive mode. However, if the structure experiences tension and bending, this deficiency could affect the mechanical capacity of the structure.

(2) *Rope anchor.* Considering the mechanical behaviour and the execution of the snow-ice foundation, the present method which anchors the guy rope to the steel bar staked into the ground is not rational. It seems that, instead of the steel bar, log timbers along the periphery are better for rope anchoring.

(3) *Filling up the space between membrane and foundation.* Because of cutting into the SP boards by the ropes, some pieces of the boards were impossible to reuse.

4.2. Creep test

4.2.1 Method of measurement

As shown in Fig. 21, nineteen points for measureing displacements were prepared at the inside surface of the test dome. The displacement transducers were used for points Nos. 0–15, and the dial gages were used for the remaining points. The displacements of points Nos. 0–14 indicate vertical displacements, and those of points Nos. 15–18 indicate normal displacements. The hanging method was adopted so as to easily measure the vertical displacements at the central parts of the dome. This method seems to be available more and more when the tested structure is getting large. The configura-

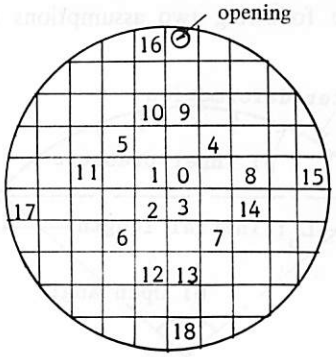

Fig. 21. Point Nos. for measuring displacement: Nos. 0–15, disp. transducer; 16–18, dial gage; 0–14, vertical disp.; 15–18, normal disp.

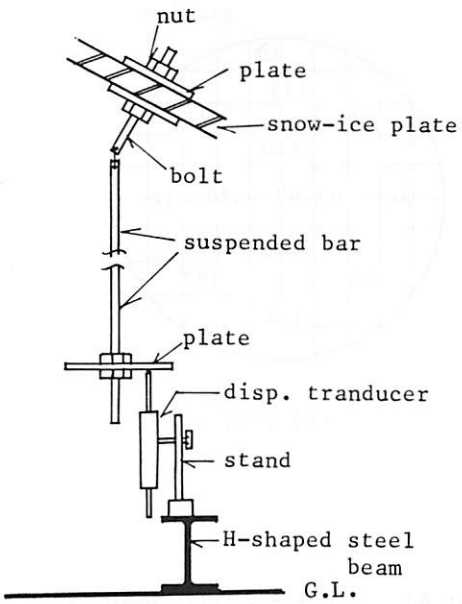

Fig. 22. Configuration of hanging method.

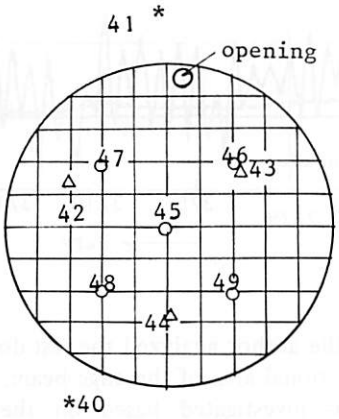

Fig. 23. Point Nos. for measuring temperature; ○ – snow-ice temp., △ – inside temp., * – outside temp.

tion of the hanging method is shown in Fig. 22.

Figure 23 shows ten points for measuring temperature. Two points are outside, three inside, and five snow-ice temperatures were measured by copper–constantan thermocouples. Displacements from points Nos. 0–15 and all temperatures were recorded automatically by a programmable data logger at adequate intervals (2,3 h) from the beginning to March 20. Figure 24 shows the inside of the dome under measurement.

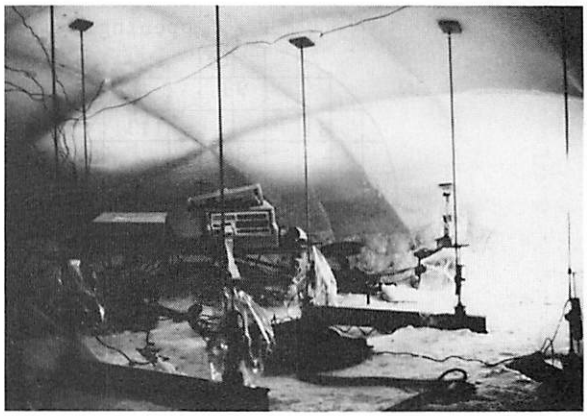

Fig. 24. Inside view under measurement.

4.2.2. Method of loading

Snow load was applied to the test dome. The snow was blown onto the dome by the snow-plow at the beginning stage. Figure 25a shows snow loads at several points measured by a thin wall sampler at that time. After that, snow load increases somewhat because of snowfall as shown in Fig. 25b. Figure 25 shows that the load distribution is not uniform because of unskilled blowing and the wind effect. According to Asahikawa Observatory's meteorological data, precipitation from January 20 to March 20 was 69.5 mm, and this value corresponds to a load of 69.5 kg/m^2. Therefore, in this test the snowfall load is lower than the blown snow load during the measurement.

4.2.3 Results and discussions

Figure 26 shows three temperature–time curves. T_{out}, T_{in} and T_{ice} are outside, inside and snow-ice temperature at representative points 40, 44 and 45, respectively. T_{in} and T_{ice} are higher and change more slowly than T_{out} due to the thermal insulation effect of snow and snow-ice, as in the previous study on the 5-m span ice dome. Rise in T_{ice} is not desirable in view of the creep behaviour. On the other hand, a high T_{in} gives a more comfortable environment. When T_{ice} and T_{in} are too high, it is easy to decrease by enlarging the opening with a stiffened edge beam if T_{out} is lower. Although T_{out} often rose to more than 0°C since the beginning of March, T_{in} and T_{ice} were still below 0°C and the dome did not collapse immediately. In fact, it was April 7 when the dome collapsed.

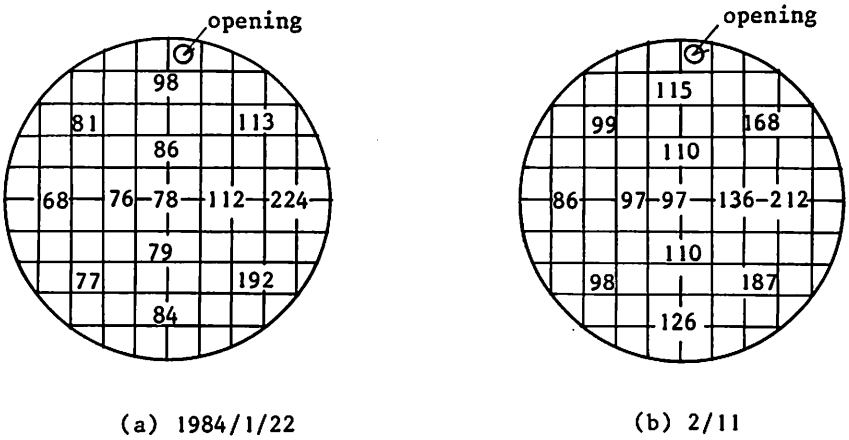

(a) 1984/1/22 (b) 2/11

Fig. 25. Observed snow load (kg/m²).

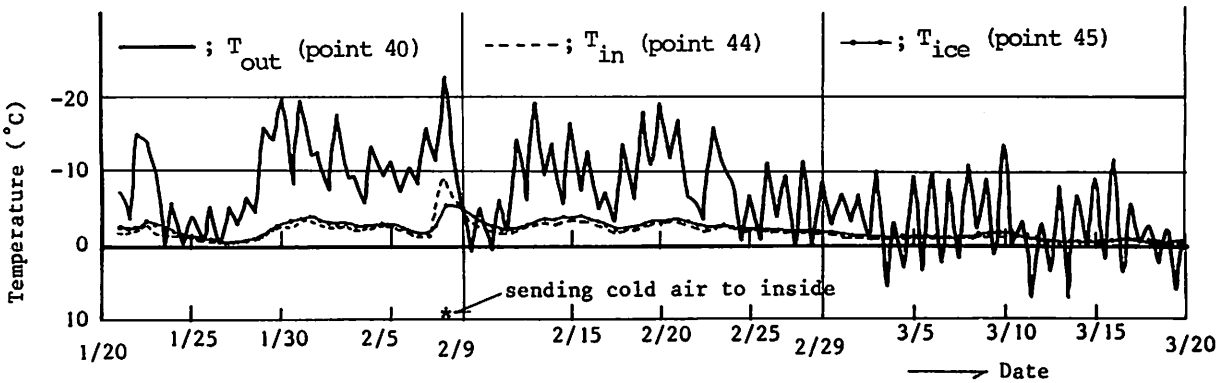

Fig. 26. Temperature–time curves.

Figure 27 shows displacement–time curves from the beginning to March 20. Points Nos. 5, 7 and 12 caused trouble in the course of measurement, and the displacement transducers were set again. Therefore, only the displacements at Nos. 5, 7 and 12 do not indicate displacements from the start. Taking a broad view of Fig. 27, the deformation grows linearly with time from the start (January 20) to the end of February, and then accelerates. Observed displacements of the points Nos. 15–18, on peripheral parts of the test dome, were one-third of those at the central parts during the steady creep stage. When the boundary is pinned or clamped, peripheral displacements are about 1/10th of the central displacement due to the linear analysis shown in a preceding paper (Kokawa and Hirasawa, 1983). Therefore, the author analyzed the test dome considering the sectional area of the edge beam. The linear analysis was investigated based on the following mathematical model. The average thickness is 12.5 cm, and the density of the snow-ice material is 0.85 g/cm³. The radius of the dome is 7.65 m as described in section 4.1.2, and the open angle is 98.8°. The sectional area of edge beam is 0.4 m² (50 cmX80 cm). The snow load is considered to be a dead load, its unit weight being 110 kg/m². As a result of this analysis, there existed the following relation between the creep coefficient η and the incremental displacement at the center $\Delta\delta_c$ (mm) in a day

$$\eta = 9.77 \cdot 10^{-10}\ \Delta\delta_c \quad (\mathrm{cm^2/kg \cdot s^{-1}}) \qquad (11)$$

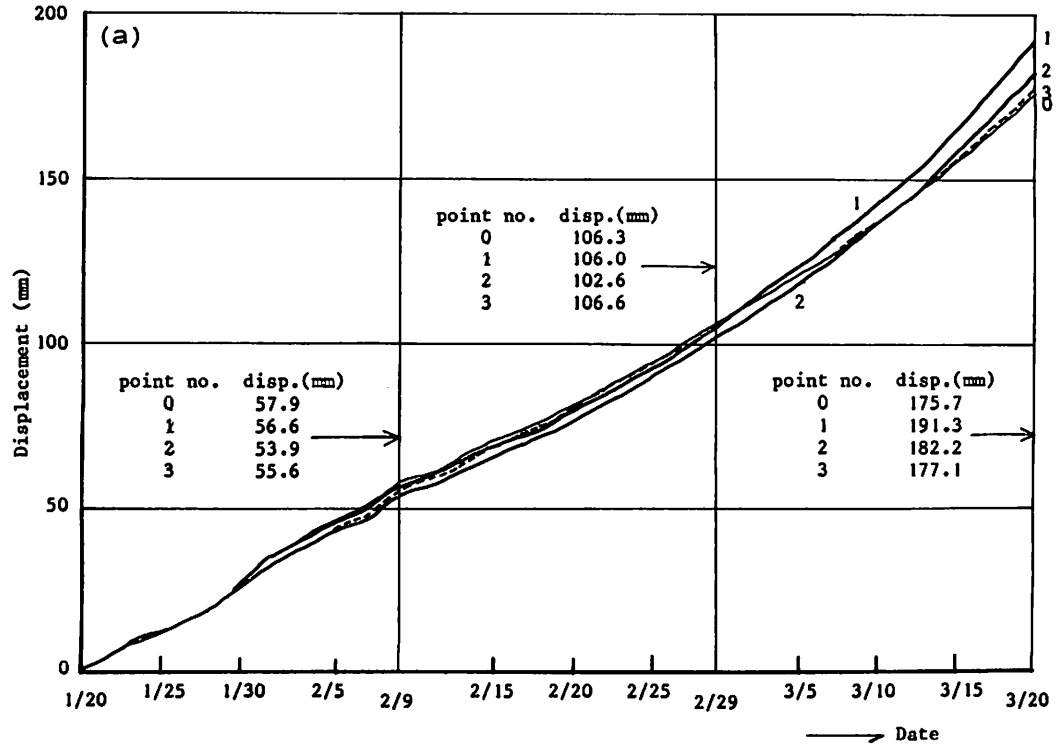

Fig. 27a. ($\delta_0 - \delta_3$)–time curves.

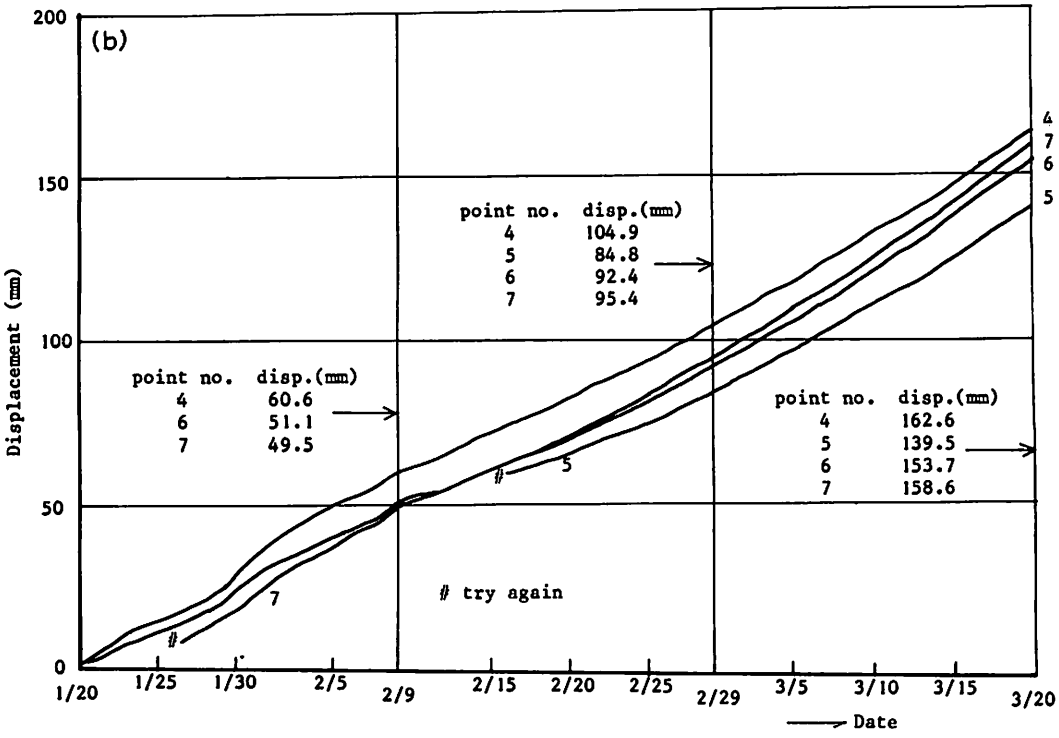

Fig. 27b. ($\delta_4 - \delta_7$)–time curves.

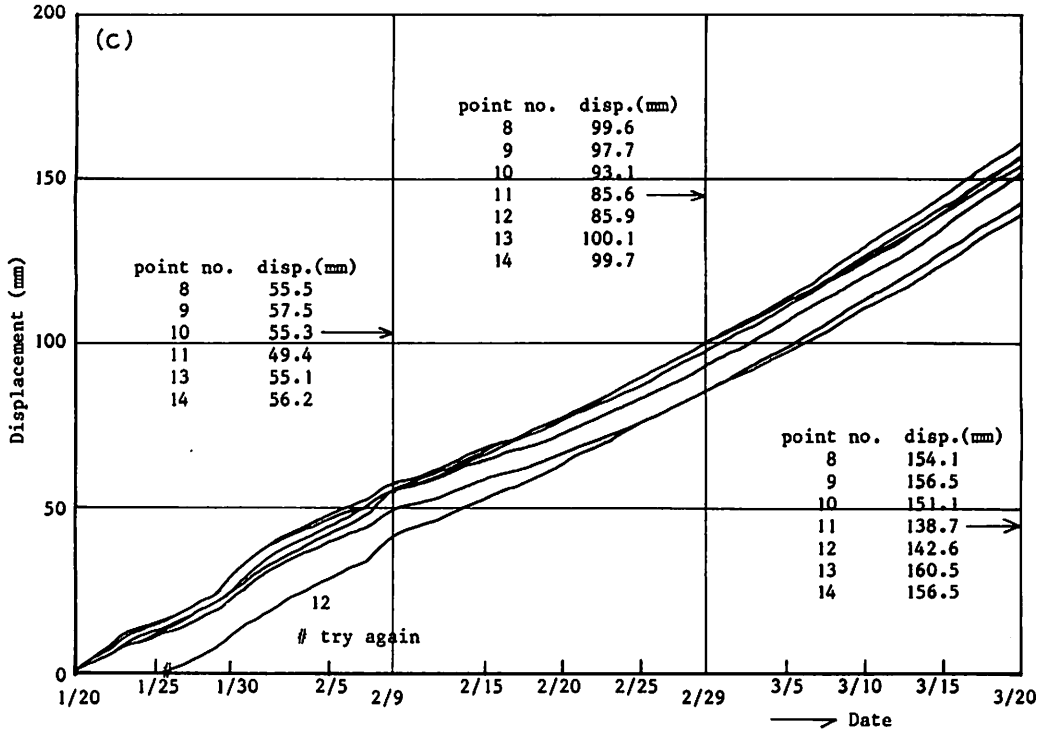

Fig. 27c. ($\delta_8 - \delta_{14}$)–time curves.

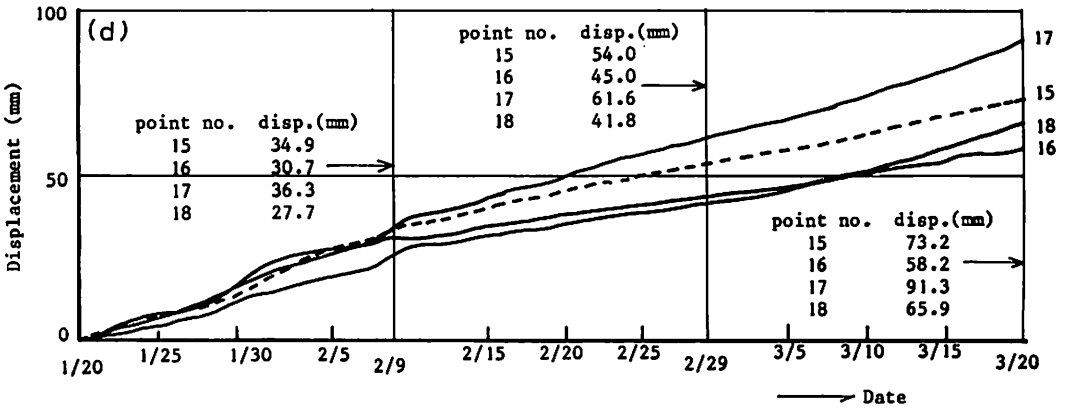

Fig. 27d. ($\delta_{15} - \delta_{18}$)–time curves.

If $\Delta\delta_c$ is 2.2 mm/d, η becomes $2.16 \cdot 10^{-9}$. The value of η is lower than the described value for the 5-m ice dome, perhaps because of the humped surface effect. A humped shell improves the structural capacity by increasing the equivalent inertia as compared with the usual monocoque shell. The qualitative estimation of the humped effect is a very important problem to be solved in the future.

As shown in Fig. 26, cold air was blown into the dome by the sirocco fan on February 8 in order to check the thermal effect. As a result of this experiment, it was shown that the rate of the observed

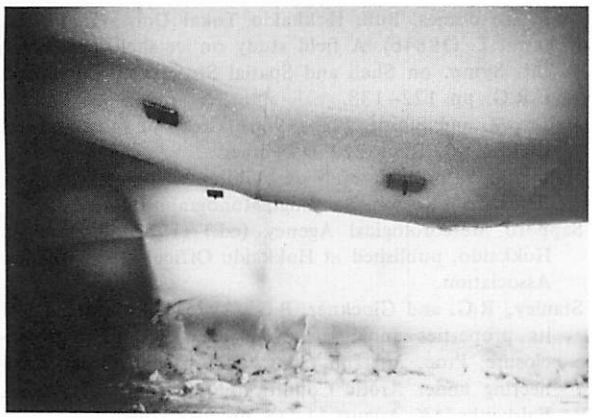

Fig. 28. Deformation at onset of collapse.

displacement is large when T_{ice} falls for a short time, and small when it rises. If T_{ice} changes sharply, the thermal deformation is larger than the creep deformation.

The central deformation accelerates gradually with time from the beginning of March. The rate of displacement at point No. 1 is 5.3 mm/d at the end of measurement. It appears that this is due to the increase of η by rising T_{ice}, the increase in load due to snowfall and the geometrical nonlinearity. On the other hand, the rate of the peripheral displacements did not vary with time.

After the measurement, on March 20, the structural behaviour was observed by eye up to the collapse. The deformation near points Nos. 1 and 2 where the snow load is comparatively small as shown in Fig. 25b, increases suddenly, and the occurrence of the antisymmetrical mode was observed at about a week before the collapse. At the onset of the collapse, the deformation was about 100 mm which means 8 times the shell thickness, as shown in Fig. 28. It indicates that the snow-ice structure is more ductile than expected. In other words, the collapse does not occur abruptly, and we have enough time to predict the danger of collapse

5. CONCLUSION

This paper has described two field tests on ice shells performed at the University of Hokkaido Tokai in Asahikawa.

The first one was an experimental study on the creep collapse of a 5-m span ice dome produced by spraying snow and water, under the concentratedly distributed load, carried out during the winter of 1981–1982. Based on the creep coefficients inferred from the observed displacements and linear shell theory, the collapse time, load and dimensionless experimental creep buckling value α_{cr} were computed. As a result, α_{cr} was 63% of the dimensionless classical buckling value as a standard value, and it was found that evaluation of the creep buckling collapse is one of the most important investigations in the design of ice shell structures.

The second one was a field study on both the construction technique and the creep test of the ice dome with 10 m span carried out during the winter of 1983–1984. The model was constructed by the following method: inflating a membrane bag covered with rope by sirocco fan and blower, spraying it with snow by snow-plow and tap water with an adjustable nozzle, solidifying the snow-ice sherbet on it, then removing the bag and ropes for reuse. This method satisfies fundamentally the facility of a rapid, easy and economical construction, though some minor imrovements are needed. After completion, inside intersecting points of the domes were measured, and they agreed with values computed by a simplified method. Subsequently, a creep test was carried out under snow load, and structural behaviour up to collapse was examined. It is gathered from the creep test that the ice shell structure is very ductile, and the humped shape will bring an improvement in structural integrity.

Based on the results of these studies, the production of 20–30-m span ice shells may be practicable.

ACKNOWLEDGEMENTS

This work was made possible by the financial supports from Grant in Aid for Scientific Research of Ministry of Education and Hokkaido, Research of Life in Northern Japan Hokkaido Tokai University and Grant in Aid for Encouragement Research of Tokai University.

The author wishes to thank Mr. Isamu Hirasawa, Assoc. Professor of Hokkaido Tokai Univ., Mr. Kōji Watanabe, Mr. Seiichi Takahashi and Mr. Takashi

Yoshida, students of Hokkaido Tokai Univ., for their valuable cooperation.

REFERENCES

Gerdeen, J.C. and Sazawal, V.K. (1974). A review of creep instability in temperature piping and vessels. WRC Bull. pp. 33–56.

Hirasawa, I. and Kokawa, T. (1984) On the creep behaviours of ice domes with span 2 m. Bull. Hokkaido Tokai Univ., 5: 7–15.

IL 9 (1976). Pneus in nature and technics. Rept. Inst. for Lightweight Structures, University of Stuttgart, pp. 118–120.

Ishii, K. (1977). Pneumatic Structures, Kogyo Chosakai, pp. 266–267.

Isler, Von H. (1979). Eis-Versuche, 2te Internationalen Symposium "Weitgespannte Flächentragwerke", Universität Stuttgart.

Kokawa, T. and Hirasawa, I. (1983). On the behaviour of ice domes under short-term loading. Bull. Hokkaido Tokai Univ., 3/4: 77–85.

Kokawa, T. (1983a). Experimental study on creep buckling collapse of ice domes with 60 cm span. Japan NCTAM, 33: 151–152.

Kokawa, T. (1983b). A study on ice shell. Proc. Japan Soc. Snow and Ice Annual Meeting, p. 108.

Kokawa, T. (1984a). Axisymmetric creep buckling analysis of ice domes. Bull. Hokkaido Tokai Univ., 5: 17–24.

Kokawa, T. (1984b). A field study on ice shell. Proc. 25th Int. Symp. on Shell and Spatial Structures, Dortmund, F.R.G., pp. 122–138.

Mellor, M. and Smith, J.H. (1966). Creep of snow and ice. CREEL Res. Rept. 220, December.

Mellor, M. (1968) Methods of building on permanent snow fields. Cold Regions Sci. Eng., Monograph III-A2a.

Sapporo Meteorological Agency (ed.) (1982). Climate in Hokkaido, published at Hokkaido Office, Japan Weather Association.

Stanley, R.G. and Glockner, P.G. (1975a). Reinforced ice: its properties and use in constructing temporary enclosure. Proc. 3rd Int. Conf. on Port and Ocean Engineering under Arctic Conditions, University of Alaska, Fairbanks, AK, August 11–15, pp. 295–299.

Stanley, R.G. and Glockner, P.G. (1975b). The use of reinforced ice in constructing temporary enclosures. Marine Sci. Commun., 1(6): 447–462.

Stanley, R.G. and Glockner, P.G. (1977). Some properties of reinforced ice. In: M.B. Ives (Ed.), Proc. Conf. on Materials Engineering in the Arctic, ASM, Metals Park, OH, pp. 29–35.

Timoshenko, S.P. and Woinowsky-Krieger, S. (1959). Theory of Plates and Shells. McGraw-Hill, London, 2nd, ed., pp. 429–465.

Timoshenko, S.P. and Gere, J.M. (1961). Theory of Elastic Stability. McGraw-Hill, London, 2nd ed., pp. 512–519.

Tokyo Astronomical Observatory (ed.) (1982). A chronological table of science. Maruzen, p. 472.